



UNIVERSITY OF LEEDS

This is a repository copy of *Suitability of excavated London Clay as a supplementary cementitious material: Mineralogy and Reactivity*.

White Rose Research Online URL for this paper:

<https://eprints.whiterose.ac.uk/204662/>

Version: Accepted Version

Article:

Dhandapani, Y. orcid.org/0000-0001-9687-5474, Marsh, A.T.M. orcid.org/0000-0002-5603-4643, Rahmon, S. et al. (3 more authors) (2023) *Suitability of excavated London Clay as a supplementary cementitious material: Mineralogy and Reactivity*. *Materials and Structures*, 56. 174. ISSN 1359-5997

<https://doi.org/10.1617/s11527-023-02260-3>

Reuse

Items deposited in White Rose Research Online are protected by copyright, with all rights reserved unless indicated otherwise. They may be downloaded and/or printed for private study, or other acts as permitted by national copyright laws. The publisher or other rights holders may allow further reproduction and re-use of the full text version. This is indicated by the licence information on the White Rose Research Online record for the item.

Takedown

If you consider content in White Rose Research Online to be in breach of UK law, please notify us by emailing eprints@whiterose.ac.uk including the URL of the record and the reason for the withdrawal request.



eprints@whiterose.ac.uk
<https://eprints.whiterose.ac.uk/>

Suitability of excavated London Clay as a supplementary cementitious material: Mineralogy and Reactivity

Yuvaraj Dhandapani¹, Alastair T.M. Marsh¹, Suraj Rahmon¹, Fragkoulis Kanavaris^{2*}, Athina Papakosta³, and Susan A. Bernal^{1*}

¹ School of Civil Engineering, University of Leeds, LS2 9JT, Leeds, UK

² Technical Specialist Services, Materials, ARUP, London, UK

³ Skanska Costain Strabag (SCS) Railways JV, London, UK

Corresponding author: Frag.Kanavaris@arup.com; s.a.bernallopez@leeds.ac.uk

Abstract

This study evaluated the potential of producing supplementary cementitious materials (SCMs) using London Clay excavated from construction activities of the High Speed 2 rail project. A trade-off between enhancing reactivity versus decomposition of impurities (e.g., pyrite, carbonates) present in different London Clay samples was considered in selecting the calcination temperature. The additional reactivity obtained by calcining at 800°C is deemed to be worth the cost of the small additional process emissions from decomposition of carbonate minerals. Blended cement formulations were developed with the produced SCMs, with replacement levels of 50 and 70 wt.%. The optimal gypsum dosage was found to be 1 wt.%, which resulted in improved reaction kinetics at early ages. Mortars produced with these binders developed ~50 MPa compressive strength after 90 days of curing even with 70 wt.% replacement, which is sufficient for potential production of low to medium strength concretes. These findings demonstrate the excellent potential of London Clays for SCM production and present a systematic approach for characterisation, processing and utilization of excavated mixed clays obtained from infrastructure projects.

Keywords

Excavated material; Calcined clays; Supplementary cementitious materials; Reactivity

33 1 Introduction

34 The construction industry faces many challenges to reduce its environmental impacts,
35 including reducing the volume of construction waste, and particularly the volume of waste sent
36 to landfill. In Europe, excavated soils are the largest stream of construction waste, estimated
37 to be <500 MT/year [1]. In the UK, there is a target to reduce excavation soil sent to landfill by
38 75% by 2040, and zero soil to landfill by 2050 [2]. Whilst some of this material can be reused
39 for geotechnical activities elsewhere on site, transportation of excavated soil to landfill is still
40 a common practice [3]. Volumes of excavated material are particularly large for major
41 infrastructure projects involving tunnelling – hundreds of megatonnes of excavated material
42 are forecast to be generated over the next 50 years [4]. Where excavation is carried out in
43 urban areas, transport of excavated soil out of the site can add disruption to local residents.
44 The overall management of excavated soil can be improved by increasing their use in
45 construction materials [5].

46 Another challenge is to reduce the embodied carbon of construction, with particular scrutiny
47 on concrete. In the UK, the Low Carbon Concrete Group roadmap targets net zero emissions
48 from concrete production by 2050, with at least a 50% reduction to be achieved by 2050 [6] .
49 One of the fastest ways to decrease the carbon footprint of cement is to decrease the clinker
50 content with higher substitutions of supplementary cementitious materials (SCMs) [7]. Blast
51 furnace slag and fly ash remain the most commonly used SCMs in the UK. However, falling
52 domestic supply and an increased reliance on imports are expected to reduce supply chain
53 resilience and increase prices in the coming years [8]. The use of calcined clay in binary and
54 ternary forms (with limestone) has the potential to reduce the CO₂ footprint of cementitious
55 materials between 30 to 50% compared to Portland clinker [9–11]. Therefore, calcined clays
56 produced from clays with low purity and/or mixed clay mineralogy are increasingly being
57 explored as an alternative to conventional SCMs. However, their variation in purity and
58 mineralogy raises questions around selection of calcination conditions to promote optimum
59 reactivity, how the properties of such calcined clays might influence fresh, mechanical or long-
60 term performance of concretes produced with them, compared with materials produced with
61 other SCMs.

62 The use of excavated clayed soils as a SCM offers an opportunity for the construction industry
63 to address the mentioned challenges simultaneously. Design of mobile calcining plants for
64 clays or soils has been proposed [12, 13]. However, an integrated calcining, grinding and
65 blending plant on-site has not yet been implemented on any major construction operations.
66 An innovative mobile clay processing facility is currently under development as part of a major
67 infrastructure project in the UK [14]. This set-up would have numerous benefits in principle,
68 including reducing the volume of excavated material sent to landfill; improving the functional
69 value of soils, relative to use in groundworks or landfill; reducing the flow of materials entering
70 and leaving the construction site, and reducing the impact of truck traffic on the
71 neighbourhood. There is increasing research interest in adopting resource recovery principles
72 in the construction lifecycle in order to reduce environmental impacts [15]; however, excavated
73 clays have received little attention so far.

74 Several routes for valorisation for excavation waste have been investigated, which include the
75 developed of supplementary cementitious materials [16–18], as fine aggregates [5, 19], for
76 development of earth-based materials [20, 21], as precursors of alkali-activated cements
77 production [22] and as raw feeds for calcium sulfoaluminate (CSA) cements production or as
78 CSA replacements [23, 24]. Wherever possible, excavation wastes should be used as raw
79 material in earth construction due to the low embodied carbon of the process, however,
80 experience has shown that excavation management is a common problem in major

81 infrastructure projects, particularly in densely populated areas, e.g., an artificial island was
82 created from waste from a past major infrastructure [25].

83 This study investigated the feasibility of producing SCMs using excavated material from
84 ongoing tunnelling works in the Greater London region, whilst the excavated material
85 predominately consists of London Clay formation. These works are linked to the first part of
86 High Speed 2 (HS2, <https://www.hs2.org.uk>), a major rail infrastructure project in the UK [26]
87 and it is estimated that over 5 million m³ of material will be excavated – the majority of this is
88 expected to be London Clay [16].

89 London Clay is the name given to the type of clays found in the London Basin geological
90 formation. They are mixed, or common, clays – their clay mineral assemblage typically
91 consists of smectite, illite, kaolinite and chlorite [27]. This diversity within the clay mineral
92 fraction makes London Clays mineralogically distinct from kaolinitic clays, which have received
93 most attention within the field of calcined clays as SCMs. Crucially, their kaolinite content is
94 relatively low – broadly within the range of 10 – 30 wt.% [27]. This is believed to be
95 disadvantageous from an SCM production perspective, as 40 wt.% of kaolinite content has
96 previously been established as the optimal amount required [28, 29] to produce blended
97 cements with equivalent strength development by 7 days to that of Portland cement systems.
98 However, the extent to which the other, less reactive clay minerals typically present in London
99 Clays (i.e. smectite, illite, chlorite) may contribute to reactivity is still an open research
100 question.

101 Non-kaolinitic clay minerals are also known to exhibit pozzolanic reactivity once calcined,
102 however, they are typically less reactive than metakaolin [30–33]. Recent work on common
103 clays from Germany determined that smectite and interstratified illite-smectite make a tangible
104 contribution to overall reactivity [34]. The only peer-reviewed study so far specifically on the
105 use of London Clays as SCMs found that calcination at 900°C for 2 hours gave the best
106 reactivity performance at 14 days and beyond, as measured by the Frattini test, portlandite
107 consumption measurements and strength activity index; however, these findings are related
108 to clays calcined in 5 cm diameter pellets in laboratory scale. Concretes with 30 wt.%
109 replacement using London Clay calcined at 900°C developed with sufficient workability (i.e.,
110 Slump class 2, 50-90 mm slump) and a satisfactory performance in terms of 90-day
111 compressive strength [18]. Another study on clays with <20 wt.% kaolinite content from a
112 variety of UK geological formations (but not including the London Clay formation) deemed
113 them to be promising as potential SCMs [35]. Whilst the small amount of literature on the use
114 of London Clays as SCMs shows promise, more research is needed in order to gain a
115 comprehensive understanding of the links between mineralogy, calcination conditions, and
116 performance in cementitious systems.

117 Beyond the role of the clay minerals, the associated minerals typically found in London clays
118 also present challenges including ensuring that sulphur-bearing phases (e.g. pyrite) in the as-
119 received material do not pose a durability threat after calcination, and ensuring that carbonate
120 minerals (e.g. calcite, dolomite) do not decompose to form problematic amounts of expansive
121 phases (e.g. free lime, periclase). Free lime and MgO are also known to cause expansion due
122 to crystallization of calcium hydroxide and magnesium hydroxide [36, 37]. Provided that
123 calcination conditions are sufficient to cause complete thermal decomposition of iron sulphide
124 phases, then their presence in an as-received clay is not problematic [38]. Aside from
125 associated minerals, it is feasible that remnants of polymer foams used for facilitating
126 excavation may be present in excavated material. It is important to assess the calcined
127 excavated materials to ensure that no such materials remain which might have a detrimental
128 effect on use in concrete.

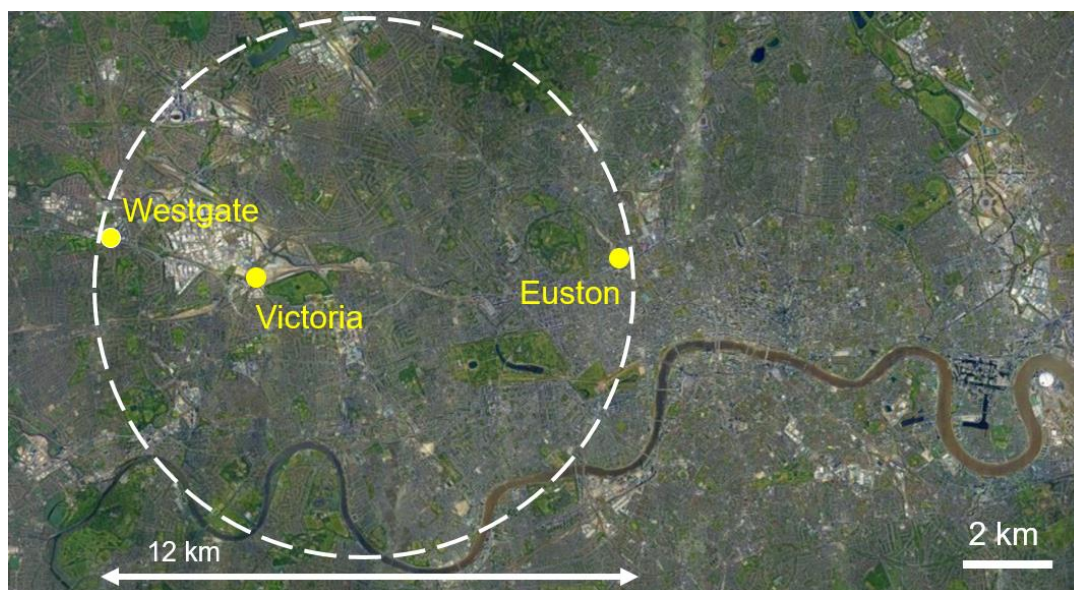
129 In this study three different sample locations of excavated London Clay were investigated.
130 These materials were selected to indicate the extent of variability of the spoils being generated
131 from HS2 excavation works in the Greater London area. Detailed characterisation of the
132 clayed soils was conducted using a multi-technique approach including X-ray fluorescence
133 spectroscopy (XRF), quantitative X-ray diffractometry (XRD) and thermogravimetry analysis
134 coupled with mass spectrometry (TG-MS). Different calcination conditions were applied to
135 these materials in order to enhance their chemical reactivity, which was determined by the R³
136 testing method. Changes in the mineralogy and structure of the excavated materials upon
137 thermal treatment was evaluated applying similar techniques to those used for characterising
138 the raw clays.

139 Blended Portland paste mixes were optimised (gypsum adjustment) and produced with high
140 replacement levels (50 wt.% and 70 wt.%) using selected calcined clays. The kinetics of
141 reaction of these mixes were determined using isothermal calorimetry. Compressive strength
142 testing in mortars specimens was also conducted.

143 2 Materials and Methods

144 2.1 Materials

145 Samples of excavated materials were sourced from three different HS2 construction sites,
146 within the Greater London area (Figure 1). All sites fell within an area with a radius of 6 km.
147 The extraction depths were 11 m for the Westgate site, 23 m for the Euston site, and between
148 3-30m depth for the Victoria site.



149
150 *Figure 1: Locations of HS2 construction sites within Greater London from where samples of*
151 *excavated material were sourced.*

152 Chemical analysis of the raw clays was conducted using X-ray fluorescence (XRF) spectroscopy,
153 carried out with a Rigaku ZSX Primus II, using a fused bead preparation method and a loss
154 on ignition (LOI) step at 900°C. The chemical oxide compositions (determined by XRF) of the
155 raw clays were broadly similar (Table 1). Differences in Al₂O₃ and CaO indicated potential
156 small differences in quantities of clay minerals and carbonates.

157

158

Table 1: Oxide compositions of the raw clays, determined by XRF.

Clay ID	SiO ₂	Al ₂ O ₃	Fe ₂ O ₃	K ₂ O	MgO	CaO	TiO ₂	SO ₃	Na ₂ O	P ₂ O ₅	Other (<0.1 wt.%)	LOI*
Westgate	53.51	13.89	6.10	2.74	2.62	6.30	0.81	0.96	0.33	0.21	0.24	12.30
Euston	56.97	15.75	6.37	3.31	2.86	2.04	0.91	0.91	0.46	0.18	0.26	10.00
Victoria	53.42	17.07	7.02	3.37	3.38	2.05	1.00	0.94	0.49	0.17	0.28	10.80

160 *LOI stands for loss on ignition determined at 900 °C for 2 hrs.

161 For the production of Portland blended mixes, a commercially available CEM I 42.5R Portland
 162 cement (from Cementos Alfa) and laboratory-grade gypsum (Calcium sulfate dihydrate, 99%,
 163 Alfa Aesar) were used. Visocrete 600 MK (from SIKA Ltd.) was used as a superplasticiser to
 164 increase fluidity of the mortars prepared with blends.

165

166 2.2 Methods

167 2.2.1 Processing and Calcination

168 Before describing the detailed steps of processing and calcination, a brief clarification of
 169 terminology will be given. Hereon, “as-received clay” is used to refer to the extracted material,
 170 before initial drying; “raw clay” is used to refer to the clay after being air-dried, crushed and
 171 homogenised; “calcined clay” is used to refer to the clay after being calcined in a laboratory
 172 furnace and ground in a laboratory ball mil, and “industrially calcined clay” is used to refer to
 173 the clay after being calcined in a pilot scale rotary kiln and and an industrial ball mill.

174 The as-received clay was manually broken into small pieces, and then dried out in shallow
 175 trays in 40°C oven for 24 hours to reach an ‘air dry state’ in line with BS 1377-1:2016 [39].
 176 This was necessary to allow the as-received material to be crushed and homogenised.
 177 Moisture content was measured according to BS 1377-2:1990 [40], with three samples of
 178 >30 g of material taken from different locations in the as-received clay, and dried at 105°C for
 179 24 hours. Moisture content calculated from mass loss was then expressed as a percentage of
 180 the dry clay mass.

181 Whilst most focus of the embodied carbon of calcined clays is on the heating required for the
 182 calcination step, the moisture content of clays has a substantial influence on the energy
 183 required for drying before calcination [41]. Moisture content is expressed as a percentage of
 184 the dry clay mass in the soil and the results varied between 20-45%, as summarised in
 185 Supplementary Information (Table S1). These values showed substantial variation in moisture
 186 content between the different clay sources. While it is not viable to conduct a cradle-to-gate
 187 analysis of embodied carbon, given the hypothetical nature of the processing set-up, these
 188 findings demonstrate that whilst the overall mineralogy between the clays did not vary greatly,
 189 differences in ground conditions could result in different energy demands for drying excavated
 190 material from different sources. It is also worth noting that apart from the ground conditions,
 191 the moisture content of soils/clays could be influenced by their storage conditions after
 192 excavation (i.e. exposure to rainfall), or even by drilling agents (e.g. polymer foams used to
 193 facilitate excavations).

194 The 'air dry' material was then passed through a jaw crusher (Retsch BB200) until all material
195 passed through a 10 mm sieve. This 10 mm upper size limit was based on recommended feed
196 size for a rotary kiln, to align the laboratory process with the industrial process as far as
197 feasible. A riffle box was then used to homogenise and obtain representative samples of
198 material from the whole. For generating finely powdered material for characterisation, a small
199 sample of ~1 wt.% of the whole was taken, and wet-ground in isopropanol until <125 µm.

200 Clays were calcined in a laboratory static furnace (Carbolite AAF 1100), using a dwell time at
201 peak temperature for about 1 hour, and a temperature of either 700°C or 800°C. These
202 temperatures were selected based on the range of dehydroxylation temperatures identified
203 via thermogravimetric analysis [42] (Section 3.1). Clays were loaded in shallow porcelain
204 crucibles. After calcination, the clay was then ground for 1 hour in a laboratory roller ball mill,
205 using ceramic grinding balls. This was undertaken to achieve a desirable particle size
206 distribution for supplementary cementitious materials ($d_{50} < 20 \mu\text{m}$ and $d_{90} < 100 \mu\text{m}$) that is
207 typical for use in cementitious materials [30].

208 For the development of blend formulations, about 300 kg of London Clay from the Westgate
209 site was industrially calcined (IC) in a rotary kiln (hereafter referred to as Westgate-IC). The
210 Westgate clay was selected on the basis of logistical convenience of sourcing larger quantities
211 of material within the planned works schedule. The as-received Westgate clay was granulated
212 into smaller pieces, calcined in a rotary kiln at 800°C with a residence time of 1 hour, and
213 subsequently ground in a ball mill. Figure 2 shows the size and colour of the clay at different
214 stages of pre- and post-calcination. Characterisation data for Westgate-IC is included in the
215 Supplementary Information.



216

217 *Figure 2: Photographs of the Westgate clay at various stages of the industrial calcination*
218 *process, with approximate scale bars to indicate changes in feed and particle size.*

219

220 2.2.2 Characterisation

221 After processing of the clays, the following analyses were performed:

222 XRD patterns were collected using a Panalytical Empyrean diffractometer (45 kV, 40 mA),
223 using a range of 4 – 70 °2θ, and a step size of 0.0131 °2θ. X'pert Highscore plus V5.1 was
224 used for phase identification using PDF-4+ 2022 ICDD database. Identification of mineral
225 phases was aided by reference to Kemp and Wagner [27], and mineral abbreviations were
226 used in line with Clay Minerals Society nomenclature described in Warr [43]. The
227 diffractograms obtained from XRD were used to investigate the mineral phase assemblages
228 via Rietveld refinement, using the external standard method where pure corundum (>99%
229 purity Al₂O₃) was tested separately the same conditions and used as an external standard for
230 analysis using the K-factor obtained from the standard for estimation of amorphous content.
231 Structure files from the 2022 ICDD PDF-4+ database were used for fitting. Due to lack of

232 Powder Diffraction File (PDF) structure files for the clay mineral montmorillonite, its low angle
233 ($<10^\circ 2\theta$) 001 reflection was excluded from the analysis – it was hence treated as part of the
234 background intensity. Due to limitations on the availability of structure files for 2:1 clays, the
235 structural file for a muscovite (a micaceous mineral) was used to fit the illite peaks. Hence, the
236 results for the proportions of minerals present in the bulk are semi-quantitative.

237 TG-MS measurements were conducting using a Netzsch STA 449 F5 coupled with a Netzsch
238 QMS 403D mass spectrometry unit. 20 ± 1 mg of sample was used for each measurement,
239 using an alumina crucible. Samples were evaluated between 30 to 1000°C using a heating
240 rate of $10^\circ\text{C}/\text{minute}$, under nitrogen atmosphere using a flow gas rate of 60 mL/min. Kaolinite
241 and carbonate contents of the source clays were estimated using the method described by
242 Snellings et al. [42]. For kaolinite, a threshold range of $400 - 600^\circ\text{C}$ was used for calculating
243 dehydroxylation mass loss; for carbonates, a threshold range of $600 - 800^\circ\text{C}$ was used for
244 calculating the mass loss due to thermal decomposition. Mineral content estimates were
245 calculated as wt.% values, with respect to the dry mass of each clay (defined here as the mass
246 at 250°C). Estimates of uncertainty were made by varying the threshold temperatures ranges
247 to plausible minimum ($400 - 550^\circ\text{C}$ for kaolinite, and $625 - 775^\circ\text{C}$ for carbonates, respectively)
248 and maximum ($300 - 625^\circ\text{C}$ for kaolinite, and $600 - 825^\circ\text{C}$ for carbonates, respectively)
249 ranges.

250 Particle size distribution (PSD) measurements were conducted using a Malvern Mastersizer
251 3000, using a dispersing unit at a rotation speed of 1400 rpm. An in-situ ultrasonication
252 treatment of 5 minutes was carried out before each measurement. Average values were
253 calculated for each sample from 10 measurements of 4 seconds duration. For clays, a
254 dispersal medium of dionised water was used, using a pinch of sodium hexametaphosphate
255 as a dispersal agent. The optical parameters used were refractive index = 1.56, and absorption
256 coefficient = 0.01 [44]. For the cement powder, isopropanol was used as the dispersing
257 medium, and measurement were collected using a refractive index = 1.7, and absorption
258 coefficient = 0.1 [44].

259 To determine the chemical reactivity of the calcined clays, the evolved heat method referred
260 to as R^3 test was adopted according to the ASTM C1897-20 [45] standard, using a TAM Air
261 calorimeter. The reactivity thresholds established specifically for calcined clays based on 7-
262 day cumulative heat values [46] were used to classify the calcined clays assessed in this study
263 according to their reactivity category.

264 To develop an understanding of how clay mineralogy affects calcined clays' chemical reactivity
265 determined according to the R^3 testing method, a series of reference clays were also tested.
266 C-K is a kaolinitic clay, calcined at 800°C . Supplementary information contains chemical
267 composition and thermogravimetric analysis of the C-K is made available in Table S6 and
268 Figure S1, respectively. This was selected to be a point of comparison, as it is a kaolinitic clay
269 with similar kaolinite content (~ 27 wt.%) to the three London Clays used in this study, but only
270 quartz as remaining fraction, enabling to identify the contribution of kaolinite reactivity alone.
271 In addition, a series of manufactured metakaolins were made, by blending an industrially
272 sourced, high-purity metakaolin (Imerys Metastar 501) with quartz. These were selected to
273 provide a hypothetical trend line, for how kaolinite content might be expected to influence the
274 reactivity of calcined clays. Characterisation data for these clays is provided in the
275 Supplementary Information.

276

277 **2.2.3 Blended cement formulations and compressive strength assessment**

278 Two replacement levels of industrially calcined Westgate clay (Westgate-IC) were chosen to
279 work with for mix design development: 50 wt.% and 70 wt.%. These will subsequently be
280 abbreviated as “CC50” and “CC70”. The main reasons why this research is limited to study
281 binary mixes with calcined clay are: i) Enable the higher waste clay re-utilisation possible and
282 consequently minimise the volumes of spoil ending in landfill, ii) Compliance with UK standards
283 which permits calcined pozzolana to replace up to 55% of CEM I while ternary mixes with
284 limestone are not included, and iii) Less complication on-site as using a ternary binder adds
285 greater complexity for on-site production with sourcing, grinding and blending of limestone.

286 For each replacement level, the influence of gypsum addition (0, 1, 3, 5 wt.%) on reaction
287 kinetics was investigated using isothermal calorimetry. For determining the optimal gypsum
288 addition for each calcined clay replacement level, isothermal calorimetry at 20°C was carried
289 out in a TAM Air calorimeter to study the hydration kinetics. Approximately 9 g of cement paste
290 (6 g of binder + 3 g of water) was used for the calorimetry measurements, mixed in-situ using
291 a vortex mixer for 2 min before placement inside the instrument. Gypsum addition was
292 attempted as high volume replacement is known to create additional sulphate demand. The
293 level of gypsum addition will be abbreviated as using a “-GN” suffix, where *N* refers to the %
294 of gypsum addition. Details of the blend composition is summarised in Table 2

295 *Table 2 Composition of the blends used for identification of gypsum adjustment.*

Blend ID	CEM I 42.5R (wt.%)	Calcined London Clay (Westgate-IC) (wt.%)	Gypsum (wt.%)
CC50 – G0	50	50	0
CC50 – G1	50	49	1
CC50 – G3	50	48	3
CC50 – G5	50	45	5
CC70 – G0	30	70	0
CC70 – G1	30	69	1
CC70 – G3	30	67	3
CC70 – G5	30	65	5

296

297 To assess the effect of different replacement levels of calcined clay on setting time, a
298 Vicamatic 2 (CONTROLS S.p.A.) automated Vicat tester was used to measure setting time.
299 Optimal blended formulations were then used to produce mortar specimens to determine the
300 mechanical strength development of these materials after 2, 7, 28 and 90 days’ curing.
301 Compressive strength measurements were carried out on mortar cubes (50 x 50 x 50 mm), in
302 line with BS EN 12390-3:2019 [47]. Mortar were prepared with CEN standardised sand with a
303 cement: sand ratio of 1:3 and a water to binder ratio (w/b) of 0.5. Superplasticizer was added
304 to ensure sufficient workability in the mortar based on the results reported elsewhere [48]. A
305 MATEST compression instrument was used with a loading rate at 3000 N/sec, and average
306 compressive strength values were calculated from three mortar cube specimens.

307

308

309

3 Results and discussion

3.1 Mineralogy of excavated clays

XRD patterns (Figure 3) revealed broad similarities in the mineralogy of the three raw clays. All clays contained kaolinite, as well as the 2:1 clay minerals montmorillonite and illite. Dolomite and smaller amounts of calcite were present in all three raw clays. Minor/trace amounts of pyrite were present in all three of the raw clays, and minor/trace amounts of gypsum were present in the Westgate and Euston clays. Powder diffraction details of phase used for analysis are kaolinite (powder diffraction file (PDF), #01-075-0938 and 04-013-2815), muscovite (PDF# 00-058-2035), quartz (PDF# 00-046-1045), microcline (PDF#01-076-1238), calcite (PDF# 00-005-0586), dolomite (PDF# 00-036-0426), Gypsum (PDF# 00-021-0816), albite (PDF# 04-007-5466), pyrite (PDF# 01-071-3840), rutile (PDF# 00-021-1276).

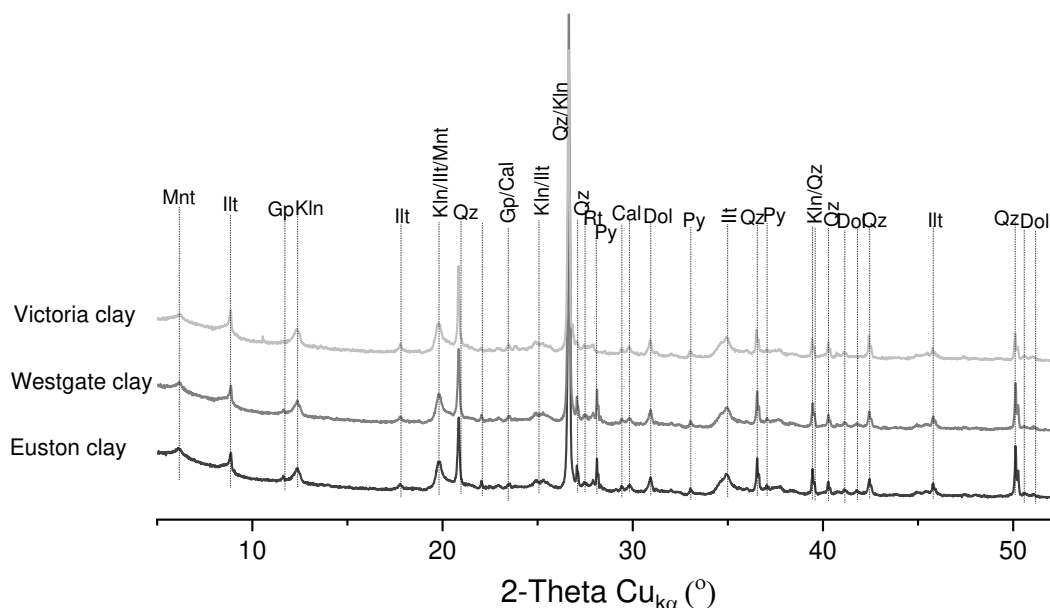
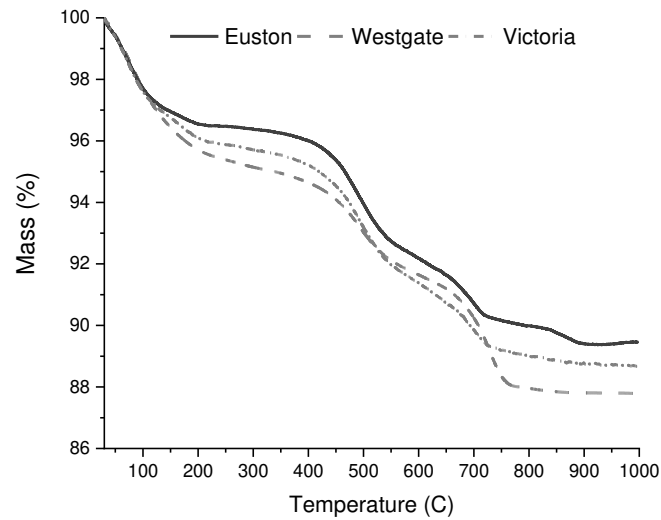


Figure 3: Cu- α XRD patterns for the raw clays. Abbreviations for clay minerals: Mnt = montmorillonite; Ill = illite; Kln = kaolinite. Abbreviations for associated minerals: Qtz = quartz; Cal = calcite; Dol = dolomite; Gp = gypsum; Py = pyrite; Rt = rutile

These clay minerals were also identified by Zhou et al. [18] studying a London Clay and in other studies on common clays [34, 35]. A wide range of associated minerals can be found in clays, depending on their formation conditions [49] – the majority of associated minerals identified here have previously been identified in a range of different occurrences of London Clay [27]. Whilst kaolinite containing quartz occurs very frequently in clays used in the SCM literature, the other clays minerals present are not so well-understood.

The TG (Figure 4) and dTG curves (Figure 5a) of the raw clays were consistent with the mineral phases identified via XRD. Evolution of H₂O (Figure 5a) over the range of 400-600°C confirmed the presence of kaolinite in all three raw clays [50]. Evolution of CO₂ (Figure 5b) over the range of 600-800°C confirmed the presence of carbonate minerals (dolomite and/or calcite) in all three raw clays [50]. The more intense weight loss in this region for the Westgate clay indicated a higher content of carbonates. Evolution of S₂ / SO₂ (Figure 5c) over the range of 450-650°C confirmed the presence of minor amounts of pyrite in all three raw clays [50], as previously identified by XRD (Figure 3). Total mass loss at 1000°C was in the range of 10.5 -

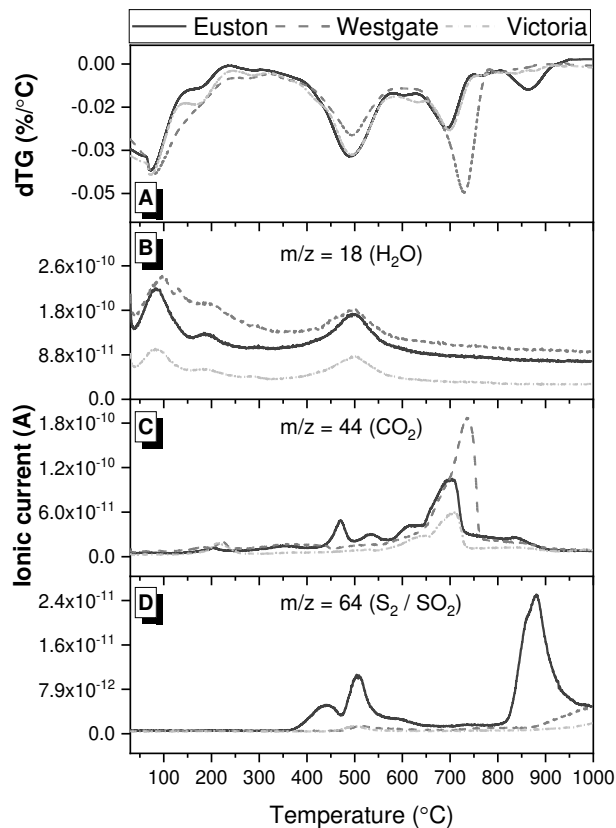
341 12.3% - this range indicates small differences in the quantities of each mineral present
 342 between the different clays.



343

344

Figure 4: Thermogravimetric curves for the raw London Clays



345

346 Figure 5: a) Differential thermogravimetric curves, and mass spectroscopy curves of b) H₂O
 347 evolution, c) CO₂ evolution, and d) S₂ / SO₂ evolution for the raw London Clays

348 Mineral phases of particular interest were kaolinite and carbonates (including both dolomite
 349 and calcite). From TG results (Figure 4), an estimate was made using mass loss from TG for

350 the quantities present in each of the three raw clays (Table S2 in the Supplementary
351 Information). Whilst the Euston and Victoria clays present similar contents of kaolinite (about
352 28%), the Westgate clay had a slightly lower kaolinite content (i.e., 22%) and slightly higher
353 carbonates content.

354 The optimal calcination temperature was anticipated to be a trade-off between an increased
355 dehydroxylation of the kaolinite as well as amorphization of the 2:1 clay minerals (beneficial
356 to reactivity), and decomposition of carbonate phases (deleterious to hydration) [18, 51].
357 Calcination temperatures of 700°C and 800°C were therefore selected, for a duration of one
358 hour in a static laboratory furnace.

359 Clays with mixed clay mineralogy and a range of associated minerals offer distinct
360 characterisation challenges compared to kaolinitic clays. Firstly, there is likely to be some
361 degree of overestimation in kaolinite content when using TG analysis. This is because non-
362 negligible mass loss arises from other clay minerals and associated minerals, which occurs in
363 the same temperature range as kaolinite dehydroxylation. This can be seen in the CO₂ and
364 SO₂ evolved gas data which confirms the decomposition of carbonate and sulphate minerals
365 in the 400-600°C temperature range. TG-MS data presented (Figure 5) shows the need to
366 critically cross-link characterisation data when adopting the mass loss method [52] to estimate
367 kaolinite content in complex clays. The same applies vice versa: it is likely that TG estimates
368 for the content of carbonate minerals is an overestimate, given that its decomposition range
369 overlaps with that of kaolinite.

370

371 3.2 Physical characteristics of calcined clays

372 On the basis of previous experience in the optimal particle size distribution of calcined
373 clays[30], upper bounds of $d_{50} < 20 \mu\text{m}$, $d_{90} < 100 \mu\text{m}$ were used as acceptable limits. All the
374 calcined clays met these particle size requirements. $d_{50} < 20 \mu\text{m}$ widely accepted range for
375 cementitious materials that are used to substitute to Portland cement. The d_{50} and d_{90} values
376 of the calcined clays after grinding are presented in Table S3, and particle size distribution
377 curves are provided in Figure S2 in the Supplementary Information file, respectively.

378

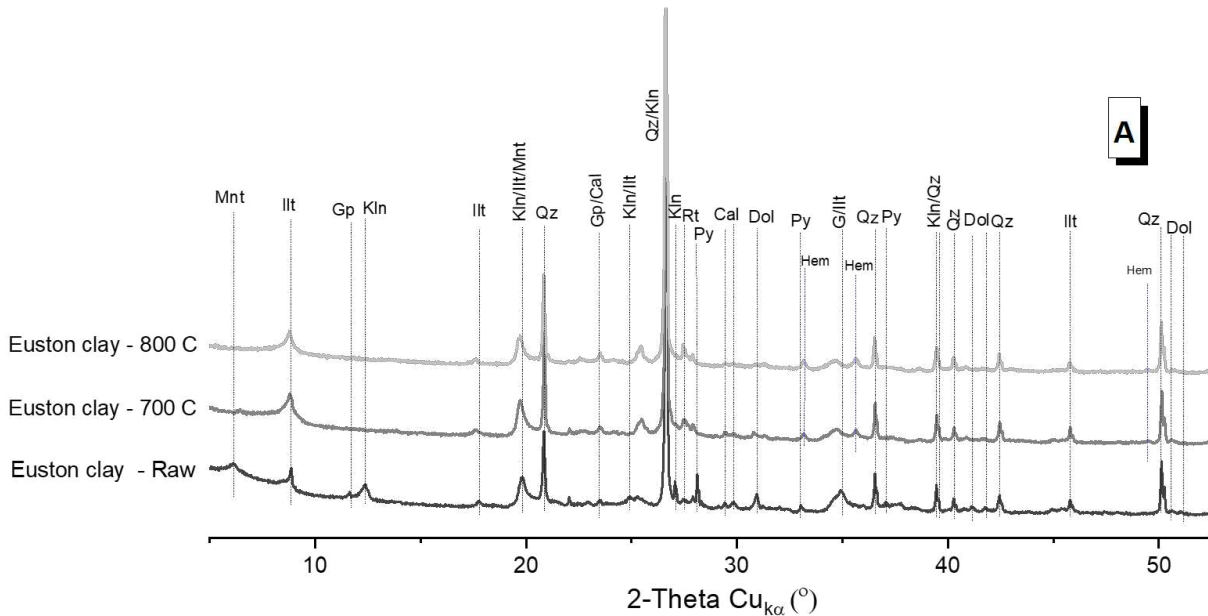
379 3.3 Mineralogy of calcined clays

380 The crystalline minerals identified in all three clays after calcination at 700°C and 800°C were
381 broadly similar, albeit with some differences (Figure 6). Dehydroxylation of kaolinite was
382 complete for all calcined clays, as seen from the absence of the kaolinite 001 peak at 12.4
383 °2 θ . A small amount of calcite was still detected after calcination at 700°C in all three clays,
384 from the doublet peaks at 29.3 and 48.4 °2 θ . Negligible calcite was detected in the Euston
385 and Victoria clays after calcination 800°C, suggesting thermal decomposition was near-
386 complete. However, a low intensity calcite peak was still detected in Westgate 800°C,
387 indicating that a small amount of calcite still remained after calcination at 800°C, probably
388 calcite formed from decomposition of dolomite to MgO and CaCO₃. Differing extents of
389 carbonate decomposition with different calcination temperatures was also observed in a
390 previous study [51].

391 No pyrite was detected in the calcined clays for all three clay sources, from the absence of
392 characteristic peaks at 28.7 and 37.3 °2 θ . Instead, peaks associated with hematite (PDF# 04-
393 015-9576) were observed at 33.1 and 35.6 °2 θ . This demonstrates the decomposition of pyrite
394 to form hematite was completed at both calcination temperatures studied. This observation
395 agrees with previous work which also showed that calcination above 650°C was sufficient to

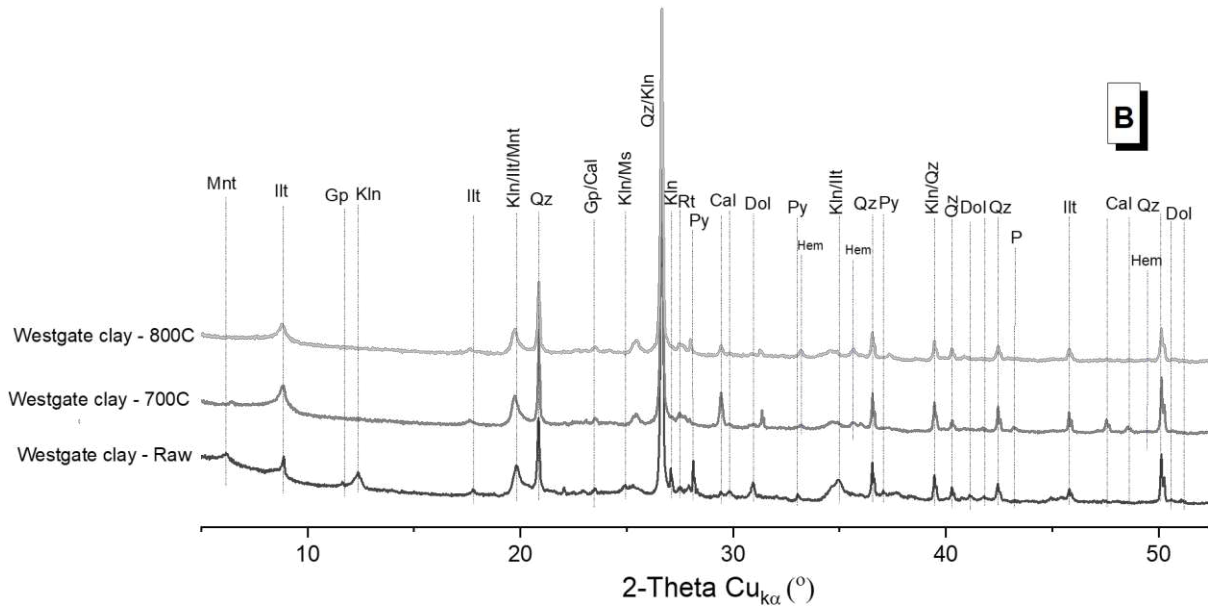
396 decompose pyrite [38]. This is an important finding which is particularly encouraging towards
 397 the adoption of calcined London Clay as an SCM in concrete, since pyritic clays are often
 398 deleterious for concrete elements [53]. Oxidation of pyrite (Fe_2S) has been known to release
 399 sulfate which could cause potential sulfate attack and also create acidic environment in the
 400 long-term exposure [54, 55]. Such sulfate attack due to pyrites present in sub-soil has been
 401 problematic in several regions of UK, US, and Canada [55, 56]. In the only previous study on
 402 calcination of London Clays [18], no calcite, dolomite or pyrite were identified in the raw clay,
 403 so there is no direct comparison to be made in this regard. This difference between the clays
 404 in these two studies is not surprising, as the presence of minor associated minerals is known
 405 to vary within the London Clay formation [27]. It is worth also noting that there might be
 406 occasions where clays are contaminated with other deleterious substances with regards to
 407 the durability of reinforced concrete, such as chlorides. Chlorides are expected to be found in
 408 clays in the vicinity of marine environments or in clays associated with saline groundwater
 409 conditions. In the particular case of London Clay considered herein, the samples investigated
 410 did not exhibit any significant chloride content, owing to the locations considered. In locations
 411 where London Clay is closer to the river Thames or Thames estuary, higher probability of
 412 chloride presence might be encountered.

413



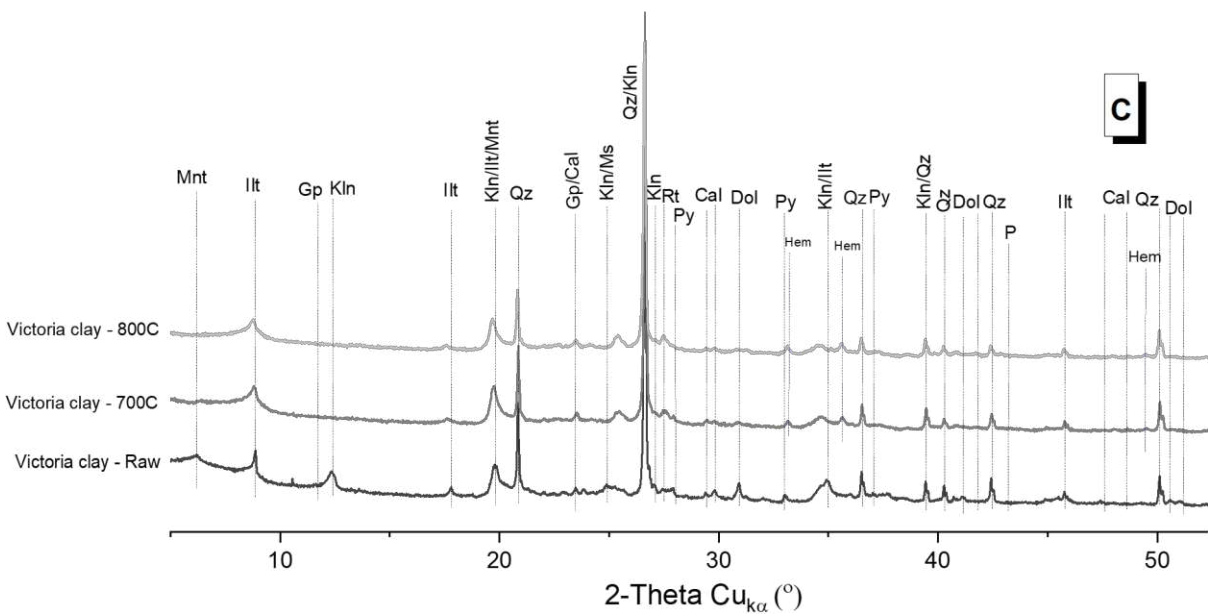
414

415



416

417

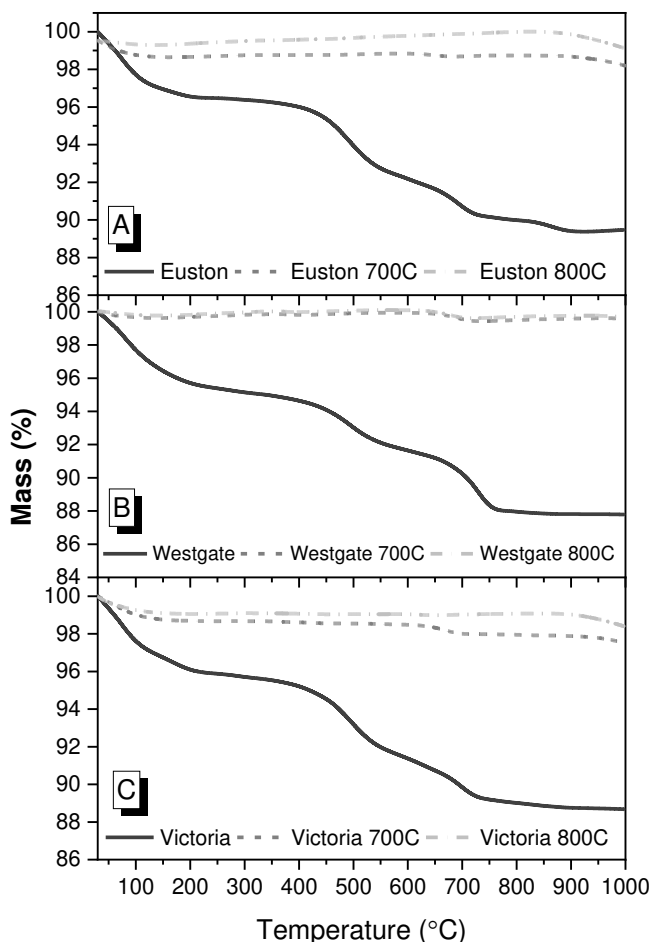


418

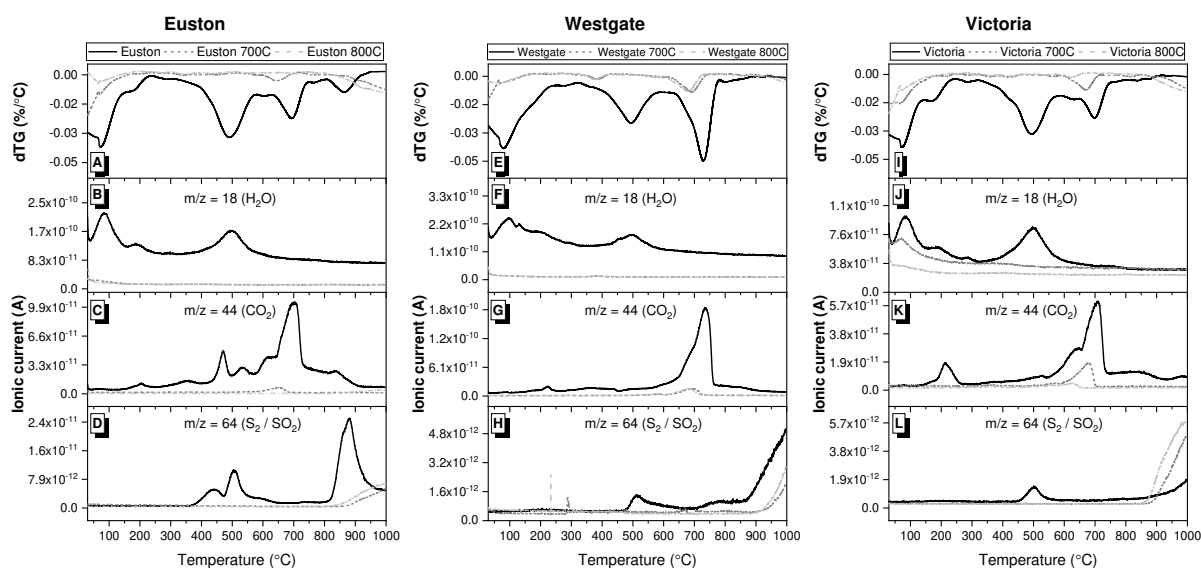
419 *Figure 6: Cu- α XRD patterns, before and after calcination, for a) Westgate clay, b) Euston*
 420 *clay, c) Victoria clay. Abbreviations for clay minerals: Mnt = Montmorillonite; Ill = Illite; Klin =*
 421 *Kaolinite. Abbreviations for associated minerals: Qtz = Quartz; Cal = Calcite; Dol = Dolomite;*
 422 *Gp = Gypsum; Py = Pyrite; Rt = Ructile; Hem = Hematite; P = Periclase.*

423 The thermogravimetric, differential thermogravimetric curves (Figure 7) and evolved gas
 424 curves (Figure 8) support the findings from the XRD analysis (Figure 6). Just as the presence
 425 of thermal mass loss event at a characteristic temperatures can indicate the presence of a
 426 given mineral [50], the absence of characteristic mass loss events can indicate the absence
 427 of a given mineral. Dehydroxylation of kaolinite was completed for all calcined clays, as seen
 428 from the absence of the peak with its centre at approximately 500°C in the dTG (Figure 8a,e,i)
 429 and H₂O (Figure 8b,f,j) evolution curves. This is consistent with the XRD results discussed
 430 above. The majority of carbonate phases (mostly dolomite) decomposed after calcination at

431 700°C [57], as seen from the reduction in magnitude of the peak centred at approximately
 432 700°C in the CO₂ evolution curves. Decomposition of carbonates seemed to be complete after
 433 calcination at 800°C in the Euston (Figure 8c) and Victoria (Figure 8k) clays, but a small
 434 amount of carbonates seemed to remain for Westgate 800°C (Figure 8g). These observations
 435 are consistent with reduction in the intensity of the reflection associated with carbonate
 436 minerals identified by XRD (Figure 6). Lastly, the conversion of pyrite to hematite in all the
 437 calcined clays was confirmed the absence of the peak centred around 500°C in the S₂ / SO₂
 438 evolution curves – this is consistent with the XRD results (Figure 6) and previous findings [38].



439
 440 *Figure 7: Thermogravimetric curves, before and after calcination, for a) Euston , b) Westgate*
 441 *and c) Victoria clays.*



442

443 *Figure 8: dTG curves and H₂O, CO₂ and S₂ / SO₂ mass spectrometry curves for a-d) Euston,*
 444 *e-h) Westgate, and i-l) Victoria clays*

445

446 Table 3 summarises the mineralogical composition of the raw and calcined clays, as
 447 determined by semi-quantitative Rietveld XRD analysis. Estimated kaolinite content of the raw
 448 clays varied from 15-18 wt.%. This is slightly lower than the range of 21-28 wt.% kaolinite
 449 content estimated from TG results (Supplementary Information - Table S2). Part of this
 450 discrepancy may potentially be explained by an overlap between dehydroxylation of kaolinite,
 451 and dehydroxylation of other clay minerals present (which cannot be fully captured in the
 452 method used here to estimate uncertainty) [42]. Thus, whilst estimates from both XRD and TG
 453 give a broadly similar range, the TG results can be considered as a more optimistic upper
 454 limit. A further challenge around characterisation is difficulties in quantifying 2:1 clay minerals
 455 using conventional characterisation methods. Values for mineral contents estimated applying
 456 quantitative XRD data need to be interpreted carefully, due to inherent limitations of this
 457 techniques and unavoidable uncertainties in the analysis process [58]. For example, the lack
 458 of suitable structural files hinders the quantification of smectite and illite clay minerals.
 459 Therefore, the estimated values for mineral contents in Table 3 should be considered as semi-
 460 quantitative.

461 Overall, the mineralogical changes in the clays after calcination were broadly similar, with
 462 some small differences. Complete dehydroxylation of kaolinite was achieved for both
 463 calcination temperatures, across all London Clays. Pyrite and dolomite were not detected in
 464 the calcined clays, due to thermal decomposition of these phases during calcination. Whilst
 465 the majority of carbonates were decomposed after calcination at both temperatures, small
 466 amounts did remain in some cases. Pyrite is a mineral known for its detrimental expansive
 467 behaviour in concrete [59, 60]. If calcination temperatures are not high enough to cause its
 468 decomposition to hematite, then it could be a cause of concern. In this study, decomposition
 469 of pyrite was achieved for both 700°C and 800°C, across all source clays. Industrial calcined
 470 (IC) Westgate soil has a marginally higher amorphous content from the larger batch of
 471 materials that was calcined industrially in a rotary kiln.

472

473
474

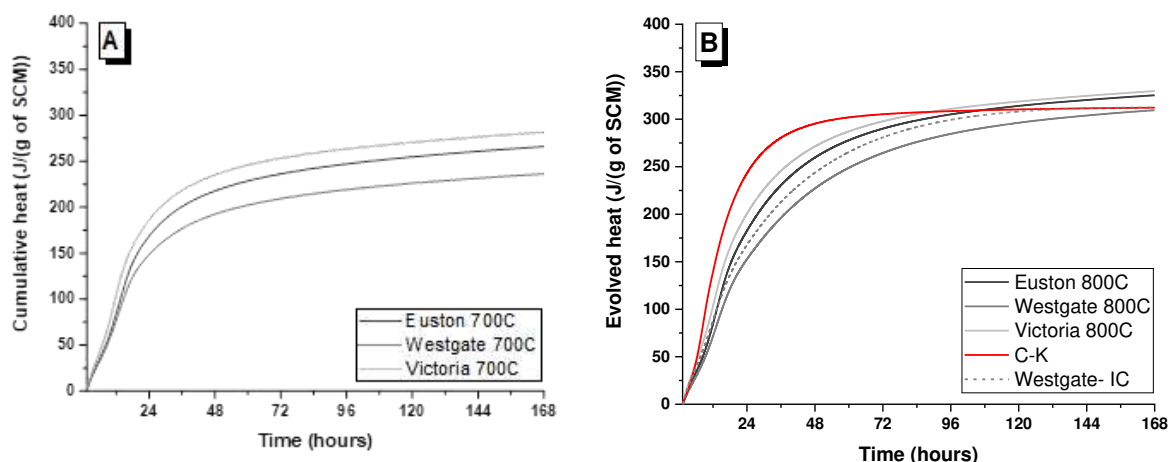
Table 3: Mineralogical composition of the raw and calcined clays evaluated. Estimated phase quantities are stated in wt.%, to a precision of 1 decimal place

	Westgate				Euston			Victoria		
	Raw	700 °C	800 °C	IC	Raw	700 °C	800 °C	Raw	700 °C	800 °C
Quartz	27.7	29.5	29.1	23.4	27.9	33.2	32.3	21.8	26	22.8
Kaolinite	15.5	0	0	0	15.1	0	0	17.9	0	0
Muscovite	45.3	40	38.4	35.3	43	33.4	35.9	45	49	43.8
Gypsum	0.9	0	0	0	0.7	0	0	0.6	0	0
Dolomite	1.6	0	0	0	1.8	0	0	1.7	0	0
Calcite	0.2	3.4	0.6	0.3	0.2	0	0	0.2	0	0
Microcline	5	9	8.6	9.8	4.6	11.3	10.4	4.5	8.3	9
Pyrite	0.6	0	0	0	0.6	0	0	0.7	0	0
Rutile	0.2	0.5	0.3	0	0.3	0.6	0.6	0.3	0.6	0.6
Hematite	0	0.9	1.2	1.0	0	1.1	1.5	0	1.3	1.5
Albite	2.4	1.5	1	0.4	2.2	2.3	1.9	1.2	2.2	2.1
Periclase	0	0	0.1	0	0	0	0	0	0	0
Lime	0	0	0.2	0.1	0	0	0	0	0.1	0.1
Amorphous content	0	15.3	20.2	29.6	3.3	18.1	17.4	5.6	12.3	20.1
Traces	0.6	-	0.3	0.1	0.3	0	0	0.5	0.2	-
Total	100	100	100	100	100	100	100	100	100	100
Goodness of Fit	2.88	3	2.75	2.24	2.93	3.3	2.97	2.6	3.2	2.7

475

476 3.4 Chemical reactivity of calcined clays

477 The R³ testing results of the calcined clays evaluated are reported in Figure 9. In each case,
478 clays calcined at 800°C exhibited slightly higher heat flow values between 1 – 4 days after
479 mixing (Figure 9a). This resulted in a modest increase in 7-day cumulative heat for clays
480 calcined at 800°C, compared to 700°C (Figure 9b). For equivalent calcination temperatures,
481 the Euston clays had slightly higher reactivity values than the Westgate clays. This could be
482 due to the Euston clay having a combination of a slightly higher kaolinite content
483 (Supplementary Information - Table S2) and slightly finer particle size distribution
484 (Supplementary Information - Table S3) compared to the Westgate clay.



485 *Figure 9: Isothermal calorimetry cumulative heat curves of all the clays as a function of the*
 486 *calcination temperature, where (A) corresponds to clays calcined at 700°C and (B)*
 487 *corresponds to clays calcined at 800 °C. C-K, a kaolinitic clay with similar kaolinite content to*
 488 *the London clays, was calcined at 800°C – it is plotted here as a reference curve.*

489

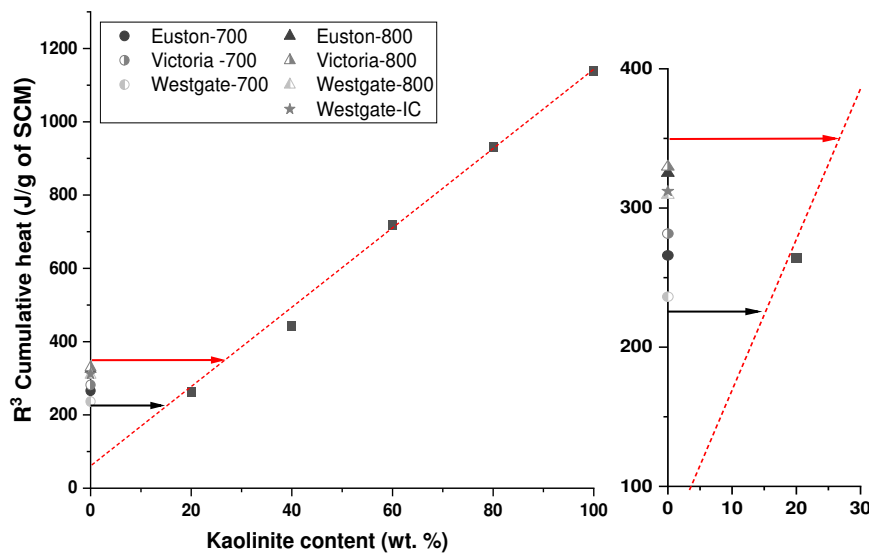
490 The 7-day cumulative heat values for all the calcined clays are listed in Table S4 in the
 491 Supplementary Information file. Robustness testing of the R³ test methods established the
 492 single operator coefficient of variance for 7-day cumulative heat to be 2.3% [61]. For the range
 493 of 7-day cumulative heat values, this corresponds to a standard deviation in the range of 5.4
 494 – 7.1 J/(g of SCM). The magnitude of the difference between the clays calcined at 800°C and
 495 700°C is 67.2 and 75.9 J/(g of SCM), for the Euston and Westgate clays respectively. Because
 496 these differences did not fall within the expected range of single operator variation, they were
 497 considered to represent meaningful differences in the measured reactivity. From the 7-day
 498 cumulative heat values (Supplementary Information - Table S4), all the calcined clays meet
 499 the 90% confidence threshold to classify as “moderately reactive calcined clays” (i.e. >190
 500 J/(g of SCM)) considering the thresholds recommended by Londono-Zuluaga et al.[46]. Out of
 501 the three clays investigated, the Westgate clay was selected to industrially produce a pilot-
 502 scale batch on the basis of logistical convenience of sourcing larger quantities of material
 503 within the planned works schedule. Given the similar mineralogy and reactivity performance
 504 of the three clays, one clay was deemed to be sufficiently representative to take forward for
 505 development of blend formulations.

506 The estimates of amorphous content from quantitative XRD (Table 3) are consistent with the
 507 observations from R³ reactivity data. R³ reactivity measurements on an industrially sourced,
 508 high purity metakaolin found the 7-day cumulative heat value to be 1150 J/g of SCM (Figure
 509 9b). The six calcined London Clays considered in this study yielded 7-day cumulative heat
 510 values in the range of 234.5 – 329.0 J/g of SCM (Supplementary Information - Table S4).
 511 These values lie in the range of 20-30% of the value for the high-purity metakaolin (as
 512 highlighted in the Figure 9). The amorphous content estimates of approximately 12-20% made
 513 via Rietveld refinement are thus broadly consistent with the observations from cumulative heat
 514 data.

515 The overall R³ results for C-K are consistent with the calcined London clays reactive content
 516 identified in this material. The reference kaolinitic clay (C-K calcined at 800°C) was chosen as
 517 the clay contained only quartz along with 27 wt.% kaolinite content. However, it is interesting
 518 to observe differences in the gradients of the cumulative heat curves over different time
 519 periods between kaolinite only clay and mixed London Clay. This highlights the difference in

520 the contribution to reactivity from reactive phases formed from different minerals i.e., only
 521 kaolinite (as in C-K) and kaolinite along with other clays minerals (as in three London clays
 522 considered in this study). The reaction kinetics during the R^3 test are slower for the calcined
 523 London Clays compared to the K-C reference kaolinite clay within the first 48 hours (Figure
 524 9b). However, beyond the first 48 hours, the calcined London Clays seem to react more quickly
 525 than the K-C reference kaolinite clay. This is likely associated with the content of 2:1 minerals
 526 in the London Clays - calcined 2:1 clay minerals are expected to exhibit slower dissolution
 527 characteristics compared to metakaolin [62, 63].

528 In order to elucidate the contribution of calcined 2:1 minerals to chemical reactivity of the
 529 calcined clays studied, a reference system was used. Testing reactivity of metakaolins of
 530 controlled purity, by blending an industrially sourced high purity metakaolin with quartz, gives
 531 a hypothetical trend line for reactivity expected from metakaolinite content alone (Figure 10).
 532 This makes possible to infer whether the presence of the calcined 2:1 clay minerals makes a
 533 contribution to reactivity above and beyond that expected from kaolinite alone.



534

535 *Figure 10: 7 day cumulative heat determined via R^3 test as a function of kaolinite content.*
 536 *Values from the calcined London Clays are plotted on the y-axis, assuming 'zero' kaolinite*
 537 *content for analysis purposes. The linear best fit line is based on the R^3 test results of tailor-*
 538 *made calcined clays containing 20, 40, 60, 80, 100% of a high-purity metakaolin, diluted with*
 539 *quartz.*

540

541 The horizontal arrows in Figure 10 extrapolate the hypothetical kaolinite content from the
 542 experimentally observed 7-day cumulative heat for the calcined London Clays. While the
 543 kaolinite content of the raw clays (determined via quantitative XRD, Table 3) were in the range
 544 of only 15-20%, calcined London Clays have a reactivity potential equivalent to kaolinite
 545 content of maximum 30% (using the trendline generated from the reference metakaolins) due
 546 to the contribution from other clay minerals. Whilst the R^3 reactivity test offer insights into the
 547 overall chemical reactivity associated with the kaolinite content in the raw clay, a degree of
 548 caution is needed in interpreting this analysis. As described in Section 3.4, the cumulative heat

549 curves in Figure 9 show that the calcined London Clays continue to react beyond 7 days, in a
550 way that the C-K reference clay did not. Given the slower reaction kinetics of mixed clays, due
551 to their 2:1 mineral content, the R³ test may slightly underestimate the reactivity of mixed clays
552 in practice, if run only for 7 days as recommended by the standard.

553 The notion of what constitutes an 'optimal' calcination temperature when processing a given
554 source clay is open to debate. R³ tests make it straightforward to make a quantitative
555 comparison of chemical reactivity at different temperatures. And yet, chemical reactivity is only
556 one of the factors that needs to be considered when deciding on a calcination temperature in
557 these systems. Two other factors are the formation of expansive phases resulting from the
558 thermal decomposition of carbonate minerals (i.e. calcite and dolomite), and the impact of the
559 resultant process emissions on the overall embodied carbon of the calcined clay.

560 Previous studies have identified a trade-off between an increased dehydroxylation of 2:1 clay
561 minerals (beneficial to reactivity), and decomposition of carbonate phases (deleterious to
562 reactivity) [18, 51]. In this study, the majority of carbonates were decomposed after calcination
563 for all clays at both 700°C and 800°C, although small amounts did remain in some cases. The
564 decomposition pathway of dolomite is distinct from calcite, and merits special attention.
565 Dolomite thermal decomposition leads to an increase in calcite content along with potential
566 formation of MgO and release of CO₂; if calcite is present in a calcined clay after calcination,
567 this could produce an aluminate-carbonate reaction leading to formation of carboaluminates
568 in hydrated cement matrix. However, negligible amounts of free lime and periclase were
569 identified in the XRD patterns after calcination at both 700°C and 800°C.

570 For the type of carbonate minerals in the three sources of London Clay studied herein, the
571 additional carbon footprint (relative to a clay without any carbonate minerals) associated with
572 the decomposition of carbonate minerals was estimated to be in the range of 24 – 42 kg /
573 tonne of calcined clay. In comparison, a typical embodied carbon of thermal treatment is
574 estimated to be at least 240 kg / tonne [41]. Therefore, decomposition of carbonate minerals
575 is likely to make a minor, rather non-negligible, contribution to the overall embodied carbon of
576 the processing of London Clay specifically and calcined clays in general.

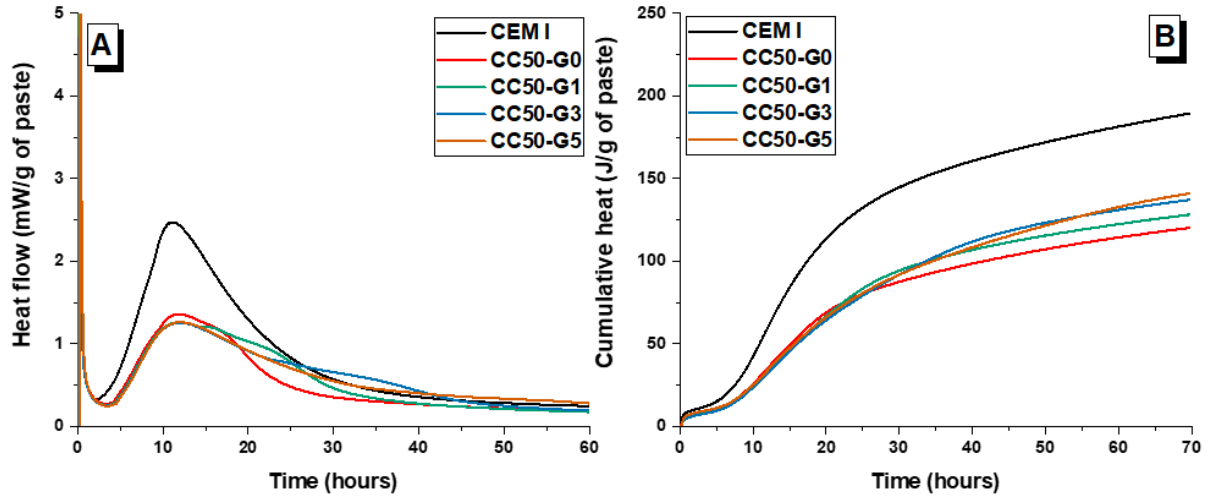
577 In the case of the sources of London Clay evaluated in this study, the minor quantity of
578 carbonate minerals (estimated <10 wt.%) suggest that there is more to gain than to lose by
579 calcining at a higher temperature of 800°C. More reactive material might lead to higher CEM
580 I replacement levels for comparable strength developments, offsetting the embodied carbon
581 associated with the decarbonation of carbonate minerals during calcination. However, this
582 should not be extrapolated as a universal finding across mixed clays. For clays with a high
583 content of carbonates and a lower content of clay minerals, it may be the case that a slightly
584 lower calcination temperature is more favourable on balance.

585

586 3.5 Blend cement formulations optimisation

587 High volume replacement of CEM I with SCMs is known to create a sulphate demand due to
588 additional aluminates and surface area introduced by the SCM that affect early age hydration
589 kinetics of clinker phases [64–66]. Hence it is important to check for sulphate demand to
590 ensure blends prepared with calcined London Clay is formulated to ensure maximum reaction
591 potential at early age. The heat flow curves for the CC50 (Figure 11a) and CC70 (Figure 12a)
592 series both exhibited a similar trend - the aluminate peak shifted to later times with increasing
593 gypsum content. At 24 hours, the pastes with 1 wt.% gypsum exhibited the highest heat flow
594 values for both CC50 and CC70 series. The heat release values were lower for the CC70
595 series due to higher replacement level of CEM I. Values of cumulative heat at 24 hours were

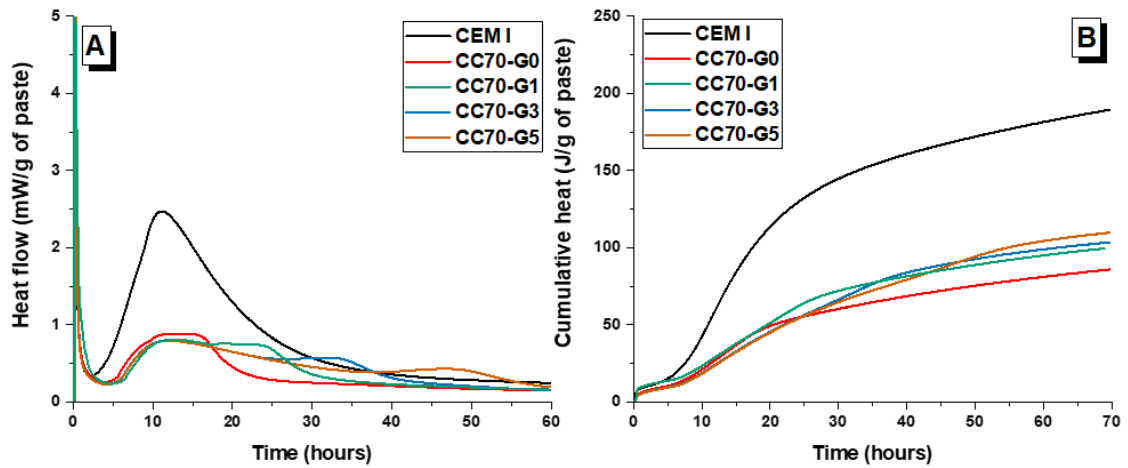
596 also marginally highest for the 1wt.% gypsum addition (Figure 13). It would therefore be
 597 expected that the 1 wt.% gypsum addition blends would exhibit higher 1-day strength. The
 598 gypsum demand did not change with the increase in replacement level from 50 to 70 wt%.
 599 This is mainly due to the relatively low metakaolin content of the industrially calcined Westgate
 600 clay.



601

602 *Figure 11: Isothermal calorimetry results of blended calcined London Clay binders showing*
 603 *the influence of gypsum addition (0 – 5 wt.%) on (A) heat flow, and (B) cumulative heat, for*
 604 *the CC-50 series*

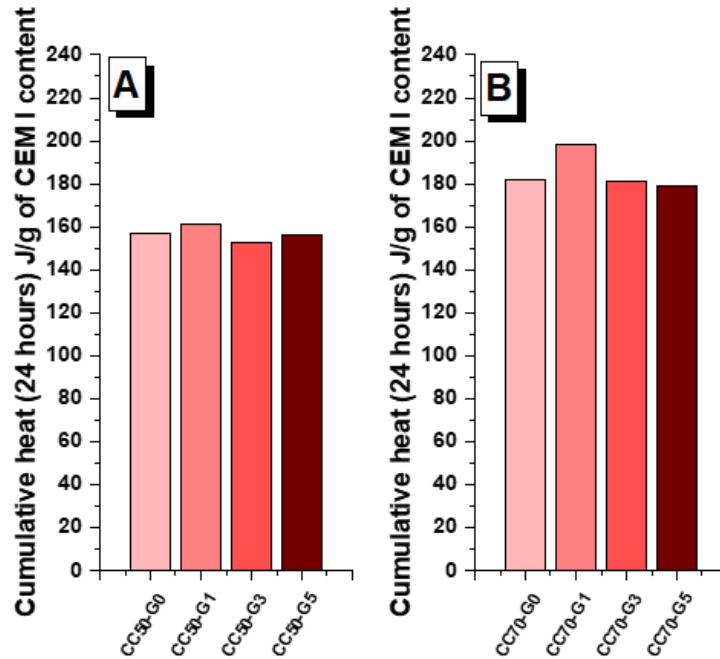
605



606

607 *Figure 12: Isothermal calorimetry results of blended calcined London Clay binders showing*
 608 *the influence of gypsum addition (0 – 5 wt.%) on (A) heat flow, and (B) cumulative heat, for*
 609 *the CC-70 series*

610

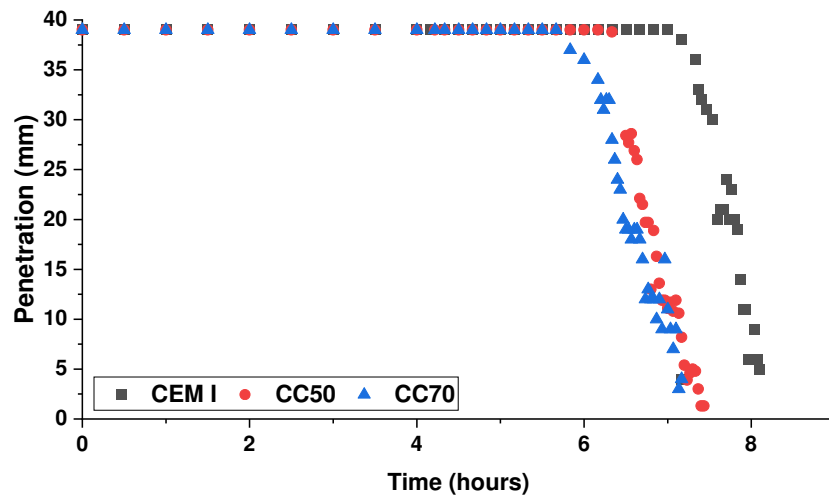


611

612 *Figure 13: Cumulative heat normalised by CEM I content at 24 hours for (A) CC-50 series,*
 613 *and (B) CC-70 series, as a function of gypsum addition in the mix (0 – 5 wt.%)*

614 The optimised gypsum addition for both CC50 and CC70 was therefore identified to be 1 wt.%.
 615 Setting time measurements were carried out for both these optimised blends (i.e. CC50-G1
 616 and CC70-G1), and compared to CEM I (Figure 14). The setting window for CC50-G1 and
 617 CC70-G1 is 6 – 8 hours. CC70-G1 is marginally faster setting than CC50-G1, and both blends
 618 exhibit noticeably accelerated setting relative to CEM I despite a delay in heat release
 619 observed from calorimetry. In this case, normalised heat flow per gram of Portland cement
 620 was able to confirm the acceleration in reaction kinetics; although heat flow per gram of paste
 621 does not showcase any acceleration of reaction. Similar reduction in setting time has been
 622 observed with other calcined clays in previous studies, attributed to the addition of calcined
 623 clay increasing the cohesivity of the mixes and heterogenous nucleation of C-A-S-H on fine
 624 calcined clay particles at early ages [67].

625



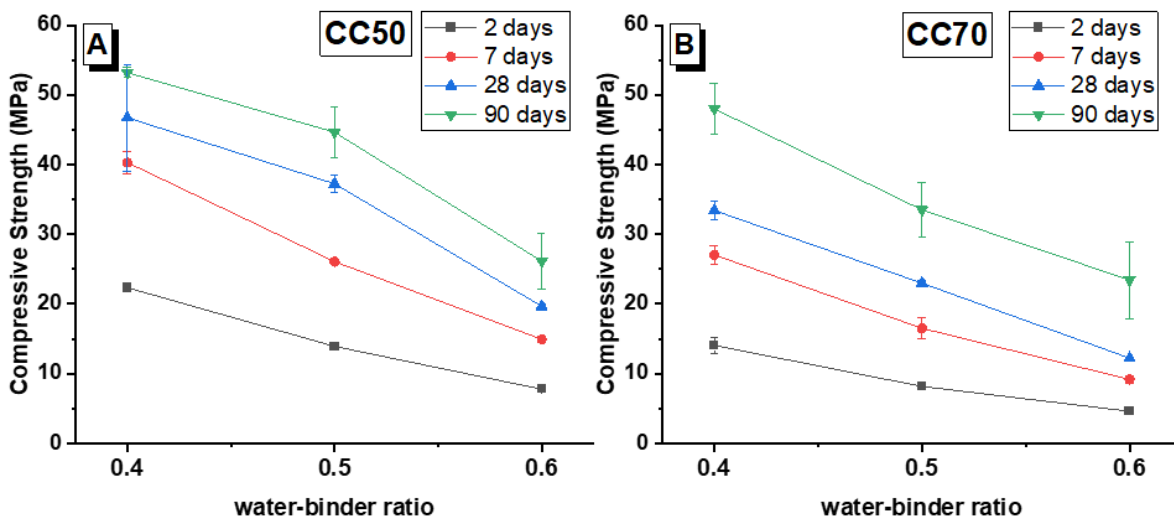
626

627 *Figure 14: Setting time curves for CEM I, CC50 and CC70 blends (both with 1% gypsum*
 628 *addition). All pastes were designed with w/b = 0.5*

629

630 **3.6 Compressive strength development**

631 The compressive strength values (Figure 15). were consistently lower for the CC70 series,
 632 compared to the CC50 series. As expected, increased w/b ratio resulted in a decrease in
 633 compressive strength, across both replacement levels. The addition of calcined clay often
 634 contributes to strength increase within 7 days of curing [29, 68, 69], and the results reported
 635 here are consistent with what has been observed in other calcined clays blended systems
 636 [67]. However, it is worth mentioning that all these studies have reported minimal strength
 637 development after 28 days while with calcined London Clay there is considerable strength
 638 development after 28 days, probably due to the slower reactivity.



639

640 *Figure 15: Compressive strength evolution as a function of curing time and w/b ratio of the*
 641 *optimised blends (A) CC50, and (B) CC70. Error bars correspond to one standard deviation*

642

643 4 Conclusions and recommendations

644 The rich variety inherent in naturally occurring clay resources offers numerous potential for
645 SCM production; but it also presents challenges. On the one hand, this study shows that
646 800°C is an effective calcination temperature for London Clays, in terms of reactivity
647 performance and avoiding potentially problematic mineral phases. However, it is also
648 highlighted that care is needed in characterisation work and decision-making. Whilst XRD and
649 TG are techniques familiar to those in the cement industry, quantifying the presence of 2:1
650 clay minerals and a range of associated minerals is not straightforward. R³ reactivity
651 cumulative heat results showcase the chemical reactivity of calcined excavated London Clay.
652 Its potential as a material suitable for SCM usage was validated by the compressive strength
653 development of blended cements produced with them.

654 London Clay samples from three different locations displayed very similar behaviour, despite
655 being sourced several kilometres away from each other. Whilst geological surveys can offer
656 valuable insights into the expected mineralogy of excavated material in a given area, detailed
657 characterisation is still necessary for quality control. Whilst many of the principles around
658 characterisation and selection of calcination temperature are more-or-less universal, these
659 formation-specific findings of the present study on London Clay cannot be transferred
660 wholesale to other geological resources (e.g., Oxford Clays, Etruria Marls) without further
661 validation. The R³ results showed that the 2:1 clay minerals present in London Clays react
662 more slowly than conventional kaolinitic clays, and that they may be making a non-negligible
663 contribution to reactivity at 7 days and possibly beyond. Therefore, it is recommended to
664 extend the R³ testing duration to 14 days for these type clays, to avoid underestimating the
665 true potential chemical reactivity of these materials.

666 Compressive strength results from optimised blended formulations indicate that high levels of
667 CEM I substitution (up to 70 wt.%) by calcined London Clays are achievable for the potential
668 production of concretes of different strength grades. Work is currently underway to develop
669 further understanding on designing blended cements, and conducting concrete mixes trials
670 using calcined London Clay SCM. Whilst low-risk applications will be the starting point for
671 concretes made with calcined London Clay, durability monitoring in natural exposure
672 conditions will still be essential for validating performance of these concretes in service.

673 The notion of 'technological robustness' will be critical to the use of excavated materials for
674 calcined clay production. The flexibility and versatility of on-site production is highly attractive
675 as an agile approach to waste minimisation and valorisation. However, this alternative
676 production model, in contrast to centralised, static production at a large clay deposit, has the
677 flipside of more attention needed to characterising the excavated materials and their variability
678 to control the quality of the materials produced from different construction sites.

679

680 Acknowledgements

681 This study was sponsored by The Skanska, Costain and STRABAG (SCS) joint venture (JV)
682 and ARUP working in partnership with HS2, through an HS2 Innovation Fund. The London
683 Clay SCM initiative was conceived and initiated by ARUP and planned and managed by SCS
684 & ARUP. The participation of Y. Dhandapani, S.A. Bernal and S. Rahmon was partially
685 sponsored by National Science Foundation (NSF) and the UK Engineering and Physical
686 Sciences Research Council (EPSRC) through the awards #1903457 and EP/T008407/1,
687 respectively. Participation of S.A. Bernal and A.T.M. Marsh was also partially sponsored by
688 though the EPSRC Early Career Fellowship grant EP/R001642/1. The donation of the
689 superplasticiser by Dr. Martin Liska from Sika UK Ltd was very much appreciated. Franco

690 Zunino, ETH Zürich along with Wolf Wichmann and Apostolos Tsoumelekas from SCS
691 Railways, London, UK are acknowledged for their involvement and discussion in the REAL
692 Project.

693

694 CRediT author statement

695

696 **Y. Dhandapani** – Investigation, Formal Analysis, Investigation, Writing – Original Draft,
697 Funding acquisition; **A.T.M. Marsh** – Investigation, Formal Analysis, Investigation, Writing –
698 Original Draft, Funding acquisition; **S. Rahmon** – Investigation, Formal Analysis; **F.**
699 **Kanavaris** – Conceptualisation, Resources; Writing - Review & Editing, Project
700 administration, Funding acquisition; **A. Papakosta** - Resources; Writing - Review & Editing,
701 Project administration, Funding acquisition; **S.A. Bernal** – Conceptualization, Methodology,
702 Formal Analysis, Writing – Review & Editing, Supervision, Project Administration, Funding
703 acquisition.

704

705

706

707 References

- 708 1. Zhang C, Hu M, Di Maio F, et al (2022) An overview of the waste hierarchy framework
709 for analyzing the circularity in construction and demolition waste management in
710 Europe. *Sci Total Environ* 803:149892.
711 <https://doi.org/https://doi.org/10.1016/j.scitotenv.2021.149892>
- 712 2. The Green Construction Board (2021) The Routemap for Zero Avoidable Waste in
713 Construction ([https://www.constructionleadershipcouncil.co.uk/wp-](https://www.constructionleadershipcouncil.co.uk/wp-content/uploads/2021/07/ZAW-Interactive-Routemap-FINAL.pdf)
714 [content/uploads/2021/07/ZAW-Interactive-Routemap-FINAL.pdf](https://www.constructionleadershipcouncil.co.uk/wp-content/uploads/2021/07/ZAW-Interactive-Routemap-FINAL.pdf))
- 715 3. Katsumi T (2015) Soil excavation and reclamation in civil engineering: Environmental
716 aspects. *Soil Sci Plant Nutr* 61:22–29. <https://doi.org/10.1080/00380768.2015.1020506>
- 717 4. Haas M, Mongeard L, Ulrici L, d'Aloia L, Cherrey A, Galler R, Benedikt M (2021)
718 Applicability of excavated rock material: A European technical review implying
719 opportunities for future tunnelling projects. *J Clean Prod* 315:128049.
720 <https://doi.org/10.1016/j.jclepro.2021.128049>
- 721 5. Magnusson S, Lundberg K, Svedberg B, Knutsson S (2015) Sustainable management
722 of excavated soil and rock in urban areas – A literature review. *J Clean Prod* 93:18–25.
723 <https://doi.org/10.1016/j.jclepro.2015.01.010>
- 724 6. Low Carbon Concrete Group, The Green Construction Board (2022) Low carbon
725 concrete routemap: setting the agenda for a path to net zero. Institute of Civil Engineers,
726 London (<https://www.ice.org.uk/media/q12jkljj/low-carbon-concrete-routemap.pdf>)
- 727 7. Shah IH, Miller SA, Jiang D, Myers RJ (2022) Cement substitution with secondary
728 materials can reduce annual global CO₂ emissions by up to 1.3 gigatons. *Nat Commun*
729 13:5758. <https://doi.org/10.1038/s41467-022-33289-7>
- 730 8. Alberici S, Beer J de, Hoorn I van der, Staats M (2017) Fly ash and blast furnace slag
731 for cement manufacturing, Department for Business, Energy and Industrial Strategy
732 (BEIS), London, U.K. Department for Business, Energy and Industrial Strategy, London,
733 U.K.
- 734 9. Sánchez Berriel S, Favier A, Rosa Domínguez E, et al (2016) Assessing the
735 environmental and economic potential of Limestone Calcined Clay Cement in Cuba. *J*
736 *Clean Prod* 124:361–369. <https://doi.org/10.1016/j.jclepro.2016.02.125>
- 737 10. Gettu R, Patel A, Rathi V, et al (2019) Influence of supplementary cementitious
738 materials on the sustainability parameters of cements and concretes in the Indian
739 context. *Mater Struct* 52: 1-11. <https://doi.org/10.1617/s11527-019-1321-5>
- 740 11. Bediako M, Valentini L (2022) Strength performance and life cycle assessment of high-
741 volume low-grade kaolin clay pozzolan concrete: A Ghanaian scenario. *Case Stud*
742 *Constr Mater* 17: p.e01679. <https://doi.org/10.1016/j.cscm.2022.e01679>
- 743 12. Salvador S, Pons O (2000) A semi-mobile flash dryer/calcliner unit to manufacture
744 pozzolana from raw clay soils — application to soil stabilisation. *Constr Build Mater*
745 14:109–117. [https://doi.org/10.1016/S0950-0618\(00\)00005-2](https://doi.org/10.1016/S0950-0618(00)00005-2)
- 746 13. Hago AW, Al-Rawas AA (2008) Design of a rotary kiln for production of Sarooj. *J Eng*
747 *Res [TJER]* 5:55–61. <https://doi.org/10.24200/tjer.vol5iss1pp55-61>
- 748 14. Kanavaris F, Papakosta A, Zunino F, Pantelidou H, Baudet B, Marsh ATM, Rahmon S,
749 Dhandapani Y, Bernal SA, Szanser J, Tsoumelekas A (2022) Suitability of excavated
750 London Clay from tunnelling operations as a supplementary cementitious material and
751 expanded clay aggregate. In: *Proceedings of the International Conference on Calcined*
752 *Clays for Sustainable Concrete (CCSC 2022)*. Sharma M, Hafez H, Zunino F, Scrivener

- 753 KL (Eds.). pp 3–4
- 754 15. Hossain MU, Thomas Ng S (2019) Influence of waste materials on buildings' life cycle
755 environmental impacts: Adopting resource recovery principle. *Resour Conserv Recycl*
756 142:10–23. <https://doi.org/10.1016/j.resconrec.2018.11.010>
- 757 16. Kanavaris F, Papakosta A (2022) Calcining excavated London Clay to produce
758 supplementary cementitious material and lightweight aggregate. *Concrete Magazine*,
759 July:40–42
- 760 17. Zhou D (2016) Developing supplementary cementitious materials from waste london
761 clay. PhD thesis, Imperial College London, UK.
- 762 18. Zhou D, Wang R, Tyrer M, Wong H, Cheeseman C (2017) Sustainable infrastructure
763 development through use of calcined excavated waste clay as a supplementary
764 cementitious material. *J Clean Prod* 168:1180–1192.
765 <https://doi.org/10.1016/j.jclepro.2017.09.098>
- 766 19. Priyadharshini P, Ramamurthy K, Robinson RG (2018) Reuse potential of stabilized
767 excavation soil as fine aggregate in cement mortar. *Constr Build Mater* 192:141–152.
768 <https://doi.org/10.1016/j.conbuildmat.2018.10.141>
- 769 20. Morel JC, Charef R, Hamard E, Fabbri A, Beckett C, Bui QB (2021) Earth as
770 construction material in the circular economy context: practitioner perspectives on
771 barriers to overcome. *Philos Trans R Soc* 376: 20200182.
772 <https://doi.org/10.1098/rstb.2020.0182>
- 773 21. Ardant D, Brumaud C, Perrot A, Habert G (2023) Robust clay binder for earth-based
774 concrete. *Cem Concr Res* 172: 107207
775 <https://doi.org/10.1016/j.cemconres.2023.107207>
- 776 22. Cristelo N, Coelho J, Oliveira M, et al (2020) Recycling and application of mine tailings
777 in alkali-activated cements and mortars—strength development and environmental
778 assessment. *Appl Sci* 10: 2084. <https://doi.org/10.3390/app10062084>
- 779 23. Julphunthong P, Joyklad P (2019) Utilization of several industrial wastes as raw
780 material for calcium sulfoaluminate cement. *Mater* 12: 3319.
781 <https://doi.org/10.3390/ma12203319>
- 782 24. Kleib J, Amar M, Benzerzour M, Abriak N-E (2022) Effect of flash-calcined sediment
783 substitution in sulfoaluminate cement mortar. *Front Mater* 9: 1035551.
784 <https://doi.org/10.3389/fmats.2022.1035551>
- 785 25. Mellings L, Limna G (2017) Crossrail learning legacy - Excavated materials story.
786 <https://learninglegacy.crossrail.co.uk/documents/excavated-materials-story/>
- 787 26. Munro A (2021) HS2 railway, UK – why the country needs it. 174:3–11.
788 <https://doi.org/10.1680/jtran.18.00040>
- 789 27. Kemp SJ, Wagner D (2006) The mineralogy, geochemistry and surface area of
790 mudrocks from the London Clay Formation of southern England. British Geological
791 Survey, Keyworth, Nottingham
- 792 28. Scrivener K, Martirena F, Bishnoi S, Maity S (2018) Calcined clay limestone cements
793 (LC3). *Cem Concr Res* 114:49–56.
794 <https://doi.org/https://doi.org/10.1016/j.cemconres.2017.08.017>
- 795 29. Avet F, Scrivener K (2018) Investigation of the calcined kaolinite content on the
796 hydration of Limestone Calcined Clay Cement (LC3). *Cem Concr Res* 107:124–135.
797 <https://doi.org/10.1016/j.cemconres.2018.02.016>

- 798 30. Fernandez R, Martirena F, Scrivener KL (2011) The origin of the pozzolanic activity of
799 calcined clay minerals: A comparison between kaolinite, illite and montmorillonite. *Cem*
800 *Concr Res* 41:113–122. <https://doi.org/10.1016/j.cemconres.2010.09.013>
- 801 31. He C, Makovicky E, Osbaeck B (1996) Thermal treatment and pozzolanic activity of Na-
802 and Ca-montmorillonite. *Appl Clay Sci* 10:351–368. [https://doi.org/10.1016/0169-1317\(95\)00037-2](https://doi.org/10.1016/0169-1317(95)00037-2)
803
- 804 32. He C, Osbaeck B, Makovicky E (1995) Pozzolanic reactions of six principal clay
805 minerals: Activation, reactivity assessments and technological effects. *Cem Concr Res*
806 25:1691–1702. [https://doi.org/10.1016/0008-8846\(95\)00165-4](https://doi.org/10.1016/0008-8846(95)00165-4)
- 807 33. Hollanders S, Adriaens R, Skibsted J, Cizer Ö, Elsen J (2016) Pozzolanic reactivity of
808 pure calcined clays. *Appl Clay Sci* 132–133:552–560.
809 <https://doi.org/10.1016/j.clay.2016.08.003>
- 810 34. Maier M, Beuntner N, Thienel K-C (2021) Mineralogical characterization and reactivity
811 test of common clays suitable as supplementary cementitious material. *Appl Clay Sci*
812 202:105990. <https://doi.org/10.1016/j.clay.2021.105990>
- 813 35. Ayati B, Newport D, Wong H, Cheeseman C (2022) Low-carbon cements: Potential for
814 low-grade calcined clays to form supplementary cementitious materials. *Clean Mater*
815 5:100099. <https://doi.org/10.1016/j.clema.2022.100099>
- 816 36. Deng M, Hong D, Lan X, Tang M (1995) Mechanism of expansion in hardened cement
817 pastes with hard-burnt free lime. *Cem Concr Res* 25:440–448.
818 [https://doi.org/10.1016/0008-8846\(95\)00030-5](https://doi.org/10.1016/0008-8846(95)00030-5)
- 819 37. Courard L, Degée H, Darimont A (2014) Effects of the presence of free lime nodules
820 into concrete: Experimentation and modelling. *Cem Concr Res* 64:73–88.
821 <https://doi.org/10.1016/j.cemconres.2014.06.005>
- 822 38. Zunino F, Scrivener K (2021) Oxidation of pyrite (FeS₂) and troilite (FeS) impurities in
823 kaolinitic clays after calcination. *Mater Struct* 55:9. <https://doi.org/10.1617/s11527-021-01858-9>
824
- 825 39. BSI BS 1377-1:2016 (2016) Methods of test for soils for civil engineering purposes.
826 General requirements and sample preparation
- 827 40. BSI BS 1377-2:1990 (1990) Methods of test for soils for civil engineering purposes.
828 Classification tests
- 829 41. Hanein T, Thienel K-C, Zunino F, et al (2021) Clay calcination technology: state-of-the-
830 art review by the RILEM TC 282-CCL. *Mater Struct* 55:3.
831 <https://doi.org/https://doi.org/10.1617/s11527-021-01807-6>
- 832 42. Snellings R, Reyes RA, Hanein T, Irassar EF, Kanavaris F, Maier M, Marsh ATM,
833 Valentini L, Zunino F, Alujas Diaz A. (2022) Paper of RILEM TC 282-CCL: Mineralogical
834 characterization methods for clay resources intended for use as supplementary
835 cementitious material. *Mater Struct* 55:149.
836 <https://doi.org/https://doi.org/10.1617/s11527-022-01973-1>
- 837 43. Warr LN (2020) Recommended abbreviations for the names of clay minerals and
838 associated phases. *Clay Miner* 55:261–264.
839 <https://doi.org/https://doi.org/10.1180/clm.2020.30>
- 840 44. Palacios M, Kazemi-Kamyab H, Mantellato S, Bowen P (2018) Laser diffraction and
841 gas adsorption techniques. In: Scrivener K, Snellings R, Lothenbach B (eds) *A Practical*
842 *Guide to Microstructural Analysis of Cementitious Materials*. CRC Press, Boca Raton,
843 FL, pp 445–483

- 844 45. ASTM C1897 – 20 (2020). Standard Test Methods for Measuring the Reactivity of
845 Supplementary Cementitious Materials by Isothermal Calorimetry and Bound Water
846 Measurements
- 847 46. Londono-Zuluaga D, Gholizadeh-Vayghan A, Winnefeld F, et al (2022) Report of
848 RILEM TC 267-TRM phase 3: validation of the R3 reactivity test across a wide range
849 of materials. *Mater Struct* 55:142. <https://doi.org/10.1617/s11527-022-01947-3>
- 850 47. BSI BS EN 12390-3:2019 (2019) Testing hardened concrete. Compressive strength of
851 test specimens
- 852 48. Dhandapani Y, Rahmon S, Marsh ATM, et al (2022) Fresh state properties of low clinker
853 cement made of excavated London Clay from tunnelling operations. In proceedings of
854 the 41st IoM³ Cement and Concrete Science Conference. Leeds, UK.
- 855 49. Alujas Diaz A, Almenares Reyes RS, Hanein T, et al (2022) Properties and occurrence
856 of clay resources for use as supplementary cementitious materials. *Mater Struct*
857 55:139. <https://doi.org/10.1617/s11527-022-01972-2>
- 858 50. Földvári M (2011) Handbook of thermogravimetric system of minerals and its use in
859 geological practice. Geological Institute of Hungary, Budapest
- 860 51. Zunino F, Boehm-Courjault E, Scrivener K (2020) The impact of calcite impurities in
861 clays containing kaolinite on their reactivity in cement after calcination. *Mater Struct*
862 53:44. <https://doi.org/10.1617/s11527-020-01478-9>
- 863 52. Avet F, Scrivener K (2020) Simple and Reliable Quantification of Kaolinite in Clay Using
864 an Oven and a Balance. In *Calcined Clays for Sustainable Concrete: Proceedings of
865 the 3rd International Conference on Calcined Clays for Sustainable Concrete* (pp. 147-
866 156). Singapore: Springer Singapore.
- 867 53. BRE Construction Division (2005) Concrete in aggressive ground - Special Digest
868 1:2005
- 869 54. Hobbs DW (2003) Thaumassite sulfate attack in field and laboratory concretes:
870 Implications for specifications. *Cem Concr Compos* 25:1195–1202.
871 [https://doi.org/10.1016/S0958-9465\(03\)00145-8](https://doi.org/10.1016/S0958-9465(03)00145-8)
- 872 55. Hobbs DW, Taylor MG (2000) Nature of the thaumasite sulfate attack mechanism in
873 field concrete. *Cem Concr Res* 30:529–533. [https://doi.org/10.1016/S0008-
874 8846\(99\)00255-0](https://doi.org/10.1016/S0008-8846(99)00255-0)
- 875 56. Duchesne J, Rodrigues A, Fournier B (2021) Concrete damage due to oxidation of
876 pyrrhotite-bearing aggregate: a review. *RILEM Tech Lett* 6:82–92.
877 <https://doi.org/10.21809/rilemtechlett.2021.138>
- 878 57. McIntosh RM, Sharp JH, Wilburn FW (1990) The thermal decomposition of dolomite.
879 *Thermochim Acta* 165:281–296. [https://doi.org/10.1016/0040-6031\(90\)80228-Q](https://doi.org/10.1016/0040-6031(90)80228-Q)
- 880 58. Snellings R (2018) X-ray powder diffraction applied to cement. In: Scrivener K,
881 Snellings R, Lothenbach B (eds) *A practical guide to microstructural analysis of
882 cementitious materials*. CRC Press, Boca Raton, FL, pp 104–176
- 883 59. Schmidt T, Leemann A, Gallucci E, Scrivener K (2011) Physical and microstructural
884 aspects of iron sulfide degradation in concrete. *Cem Concr Res* 41:263–269.
885 <https://doi.org/10.1016/j.cemconres.2010.11.011>
- 886 60. Capraro APB, Braga V, de Medeiros MHF, Hoppe Filho J, Bragança MO, Portella KF,
887 de Oliveira IC (2017) Internal attack by sulphates in cement pastes and mortars dosed
888 with different levels of pyrite. *J Build Pathol Rehabil* 2:7. <https://doi.org/10.1007/s41024->

889
890
891
892
893
894
895
896
897

898
899
900
901

902
903
904

905
906
907

908
909
910

911
912
913
914

915
916
917
918

919
920
921

922
923
924

925

926

927

928

929

017-0026-9

61. Avet F, Li X, Ben Haha M, Bernal SA, Bishnoi S, Cizer Ö, Cyr M, Dolenc S, Durdzinski P, Haufe J, Hooton D, Juenger MCG, Kamali-Bernard S, Londono-Zuluaga D, Marsh ATM, Marroccoli M, Mrak M, Parashar A, Patapy C, Pedersen M, Provis JL, Sabio S, Schulze S, Snellings R, Telesca A, Thomas M, Vargas F, Vollpracht A, Walkley B, Winnefeld F, Ye G, Zhang S, Scrivener K (2022) Report of RILEM TC 267-TRM: Optimization and testing of the robustness of the R3 reactivity tests for supplementary cementitious materials. *Mater Struct* 55:92. <https://doi.org/10.1617/s11527-022-01928-6>
62. Werling N, Kaltenbach J, Weidler PG, et al (2022) Solubility of calcined kaolinite, montmorillonite, and illite in high molar NaOH and suitability as precursors for geopolymers. *Clays Clay Miner* 70:270–289. <https://doi.org/10.1007/s42860-022-00185-6>
63. Bauer A, Berger G (1998) Kaolinite and smectite dissolution rate in high molar KOH solutions at 35° and 80°C. *Appl Geochemistry* 13:905–916. [https://doi.org/10.1016/S0883-2927\(98\)00018-3](https://doi.org/10.1016/S0883-2927(98)00018-3)
64. Andrade Neto J da S, De la Torre AG, Kirchheim AP (2021) Effects of sulfates on the hydration of Portland cement – A review. *Constr Build Mater* 279:122428. <https://doi.org/10.1016/j.conbuildmat.2021.122428>
65. Zunino F, Scrivener K (2022) Insights on the role of alumina content and the filler effect on the sulfate requirement of PC and blended cements. *Cem Concr Res* 160:106929. <https://doi.org/10.1016/j.cemconres.2022.106929>
66. Maier M, Sposito R, Beuntner N, Thienel K-C (2022) Particle characteristics of calcined clays and limestone and their impact on early hydration and sulfate demand of blended cement. *Cem Concr Res* 154:106736. <https://doi.org/10.1016/j.cemconres.2022.106736>
67. Dhandapani Y, Santhanam M, Gettu R, et al (2020) Perspectives on blended cementitious systems with calcined clay- limestone combination for sustainable low carbon cement transition. *Indian Concr J* 25–38. https://www.icjonline.com/explore_journals/2020/02/
68. Antoni M, Rossen J, Martirena F, Scrivener K (2012) Cement substitution by a combination of metakaolin and limestone. *Cem Concr Res* 42:1579–1589. <https://doi.org/10.1016/j.cemconres.2012.09.006>
69. Dhandapani Y, Sakthivel T, Santhanam M, et al (2018) Mechanical properties and durability performance of concretes with Limestone Calcined Clay Cement (LC3). *Cem Concr Res* 107:136–151. <https://doi.org/10.1016/j.cemconres.2018.02.005>